Microorganism dynamics in a mudflat during rising tide Microorganism dynamics during a rising tide: Disentangling effects of resuspension and mixing with offshore waters above an intertidal mudflat

Katell Guizien, Christine Dupuy, Pascaline Ory, Hélène Montanié, Hans Hartmann, Mathieu Chatelain, Mikhaïl Karpytchev

Running title: Microorganism dynamics in a mudflat during rising tide

Microorganism dynamics during a rising tide: Disentangling effects of resuspension and mixing with offshore waters above an intertidal mudflat

Katell Guizien[1†*], Christine Dupuy [2†], Pascaline Ory[2], Hélène Montanié[2], Hans Hartmann[2], Mathieu Chatelain[1,], Mikhaïl Karpytchev[2]**

1. **Laboratoire d'Ecogéochimie des Environnements Benthiques, Observatoire Océanologique de Banyuls-sur-Mer, UMR8222, CNRS-Université Pierre et Marie Curie, rue du Fontaulé, 66650 Banyuls-sur-Mer, France**
2. **Littoral, Environnement et SociétéS (LIENSs), Université de La Rochelle, UMR 7266 CNRS-ULR, 2 rue Olympe de Gouges, 17000 La Rochelle Cedex, France**

† These authors contributed equally to this work.

***Corresponding author: guizien@obs-banyuls.fr, Tel: +33 (0) 468 887 319, Fax: +33 (0) 468 887 395**

** Present address: Deltares, P.O. Box 177, 2600 MH Delft, The Netherlands

Keywords: microorganisms dynamics, bentho-pelagic coupling, resuspension, tidal mudflat

Abstract

Resuspension of microphytobenthic biomass that builds up during low tide has been acknowledged as a major driver of the highly productive food web of intertidal mudflats. Yet, little is known about the contribution to pelagic food web of the resuspension of other microorganisms such as viruses, picoeukaryotes, cyanobacteria, bacteria, nanoflagellates, and ciliates, living in biofilms associated with microphytobenthos and surficial sediment. In the present study, a novel approach that involves simultaneous Lagrangian and Eulerian surveys enabled to disentangle the effects of resuspension and mixing with offshore waters on the dynamics of water column microorganisms during a rising tide in the presence of waves. Temporal changes in the concentration of microorganisms present in the water column were recorded along a 3 km cross-shore transect and at a fixed subtidal location. In both surveys, physical and biological processes were separated by comparing the time-evolution of sedimentary particles and microorganisms concentrations. During a rising tide, sediment erosion under waves action occurred over the lower and upper part of the mudflat, where erodibility was highest. Although erosion was expected to enrich the water column with the most abundant benthic microorganisms, such as diatoms, bacteria and viruses, enrichment was only observed for nanoflagellates and ciliates. Grazing probably overwhelmed erosion transfer for diatoms and bacteria, while adsorption on clayed particles may have masked the expected water column enrichment in free viruses due to resuspension. Ciliate enrichment could not be attributed to resuspension as those organisms were absent from the sediment. Wave agitation during the water flow on the mudflat likely dispersed gregarious ciliates over the entire water column. During the rising tide, offshore waters imported more autotrophic, mainly cyanobacteria genus *Synechococcus* sp. than heterotrophic microorganisms, but this import was also heavily grazed. Finally, the water column became a less heterotrophic structure in the subtidal part of the semi-enclosed bay, where mixing with offshore waters occurs (50% decrease), compared to the intertidal mudflat, when resuspension occurs. The

present study suggests that this differential evolution resulted predominantly from dilution with offshore waters less rich in heterotrophic microorganisms. Indeed, any input of microorganisms accompanying physical transfers due to bed erosion or offshore waters mixing was immediately buffered, probably to the benefit of grazers.

1. Introduction

The productivity of coastal systems, especially intertidal mudflats, and their capacity to enrich adjacent terrestrial and marine zones through trophic pathways (i.e. export by mobile consumers) and hydrodynamic pathways (i.e. waves, wave-generated currents, estuarine currents and tides) is now common knowledge. The biological productivity of intertidal mudflats is due to the intense activity of benthic microorganism communities. During emersion, epipelic diatoms (microphytobenthos, MPB) form a biofilm (up to 20 mg chlorophyll *a* m^2) in the top centimeter layer of a mud surface (Blanchard and Cariou-Le Gall 1994; Blanchard et al. 1997; Herlory et al. 2004). Prokaryote communities are associated with this biofilm, and bacterial production (secondary production) can be as high or even higher than MPB production (primary production) (Cammen 1991; Garet 1996; Van Duyl and Kop 1994). Bacterial concentration is generally about 10^9 cells per cm^3 in a mudflat (Schmidt et al. 1998). Nanoflagellate concentrations range from 100 to several million cells per mL of sediment (Gasol 1993), with greater concentrations in surficial sediment (Alongi 1991). Conversely, ciliates are more abundant in fine sand (Fenchel 1969; Kemp 1988; Epstein 1997) compared to muddy sediment enriched with organic matter (Giere 1993). Viruses are also abundant in marine sediments (Danovaro et al. 2008).

Resuspension of microorganisms living either in the pore water of surficial sediment or attached to surficial sedimentary particles have been reported under tidal currents at subtidal sites (Shimeta et al. 2002). Large tidal currents in macrotidal bays are likely to induce unconsolidated sediment resuspension (Mehta et al. 1989). Yet, resuspension of sediment

across intertidal mudflats, where recurrent desiccation promoted sediment consolidation (Anderson and Howel 1984), generally requires higher shear stress than those induced by tidal current and has been mainly attributed to wave action (Bassoulet et al. 2000; French et al. 2008). However, sediment erodibility thresholds may be significantly reduced (bed friction velocity below 3 cm s^{-1}) due to macrofaunal bioturbation activity (Orvain et al. 2007).

Resuspended microorganisms may greatly affect pelagic and benthic food webs. Resuspended diatoms and autotrophic nanoflagellates may alter phytoplankton community structure, enhance phytoplankton biomass and modify the size structure of primary producers, ultimately modifying microbial food web function (Marquis et al. 2007; Ory et al. 2010). In addition, resuspended heterotrophic cells, such as nanoflagellates, prokaryotes (bacteria and archaea) and viruses, can affect the function of the food web, and favour the microbial loop or the viral shunt (Wainright 1987; Garstecki et al. 2002; Seymour et al. 2007). Furthermore, some of these resuspended microorganisms may be used as food resources for mesozooplankton and benthic suspension feeders (Carslon et al. 1984), such as oysters (Dupuy et al. 2000) and bivalve mollusks (*Scrobicularia plana*) (Hughes 1969).

Many studies have investigated the dynamics of the MPB biomass, including resuspension of these microorganisms (Lucas et al. 2000; Shimeta et al. 2002; Guarini et al. 2008). Some studies have qualitatively and quantitatively evaluated the resuspension of other microorganisms present in the intertidal mudflat. Protist and bacteria resuspension thresholds have been quantified at a subtidal coastal site with *in situ* flumes and sampling of the benthic boundary layer during tidal accelerations (Shimeta and Sisson 1999; Shimeta et al. 2002). Shimeta et al. (2003) studied the resuspension of benthic protists at subtidal coastal sites with differing sediment compositions. Other studies have explored the effects of sediment resuspension on a coastal planktonic microbial food web, either experimentally (Garstecki et al. 2002; Pusceddu et al. 2005; Wu et al. 2007) or in the field (Grémare et al. 2003). However, in field studies, resuspension is often accompanied by other physical processes, such as river

flooding and tidal rise, which require adapted sampling strategies to separate the contribution of each process.

In the current study, we applied a novel approach based on two simultaneous Lagrangian and Eulerian field surveys to disentangle the effect of resuspension and mixing with offshore waters on the dynamics of water column microorganisms during a tidal flow. The time-evolution of microorganisms, including viruses, autotrophic protists, heterotrophic protists and prokaryotes present in the water column, were carried out at one fixed location (Eulerian) and one mobile station (Lagrangian) in the Marennes-Oleron bay (French Atlantic coast). In both surveys, physical and biological processes were separated by comparing the time-evolution of suspended sediment particles and microorganisms concentrations.

2. Methods

2.1 Study site and sampling strategy

The study was carried out during the afternoon rising tide (tidal amplitude of 3.8 m) in the Bay of Marennes-Oléron (BMO) on 24 July, 2008. Located between the mainland French Atlantic coast and Oléron Island, BMO is a macrotidal bay with a tidal range up to 6 m during spring tides. This macrotidal system is influenced by continental inputs, mainly from the Charente River to the north of the BMO (monthly average discharge was 30 m^3 s^{-1} in July 2008, slightly less than the median value of 40 m^3 s^{-1} over the last ten years). The BMO covers 170 km^2, of which 60 km^2 are intertidal mudflats. The Brouage mudflat is >4 km wide, and its sediment consists of silt and clay particles (95% of <63 µm, median grain size d_{50} = 10 µm). Triplicate samples of the first 1 cm layer of sediment were taken at the end of low tide in the upper region of the mudflat (Fig. 1). Only concentrations of bacteria and viruses were assessed in surficial sediment. Two simultaneous field surveys (Lagrangian and Eulerian) were carried out to separate the effect on the dynamics of water column microorganisms of resuspension and mixing with offshore waters during tidal flow. Adopting a Lagrangian

strategy avoided transport flux gradients that occur in an Eulerian survey. Such transport flux gradients occur as the water level changes in an Eulerian survey and pelagic concentrations are generally expected to be mixed (diluted or enriched) by offshore waters in proportion to water depth. Conversely, no mixing (especially dilution) is expected in a Lagrangian survey, where the water level remains constant. In both types of surveys, temporal changes in concentrations of a group of organisms, or particulate or dissolved matter that depart from these expectations indicate an imbalance between the many biogeochemical processes that potentially affect this group (Fig. 2). For particulate matter or living low-motility cells, an overall increase in concentration indicates that either benthic resuspension or population growth dominate, whereas a decrease indicates that either sedimentation mediated by sorption on matters or population decay (e.g. grazing) dominates.

Before organizing the field measurements, a 2D barotropic model was used to compute using a backward procedure the trajectory of a drifter reaching the shore in the northern part of the Brouage mudflat (Fig. 1) at the end of the rising tide (Nicolle and Karpytchev 2007). The model used a high resolution, finite element grid and TELEMAC software to solve the depth integrated equations of Saint Venant (Hervouet and Van Haren 1994; Hervouet 2007). The Eulerian subtidal station was located at the origin of the drifter trajectory for the case of a no-wind tidal circulation in the BMO (Fig. 1).

The Lagrangian survey consisted of tracking a submerged buoy following the tidal front during the first 2 h 45 min of the rising tide over the intertidal Brouage mudflat, between 15:45 h and 18:30 h local time (Fig. 1). The tidal front travelled roughly at a speed of 30 cm s^{-1}. Cylindrical drifters (46 cm in diameter and 50 cm in height) were used to track the advancing tidal currents into the BMO. Drifter walls were made of plastic film wrapped around a thin metal rod armature and a 10 cm plastic spherical buoy was fixed on its top. The drifter was completely immersed to be directed by surface currents and the buoyant sphere which emerged from water was used to keep track of the drifter position. The drifter was

158 tracked using a flatboat which engine was stopped and left drifting for at least 5 min before
159 sampling in order to avoid bottom resuspension artefacts. Water samples were obtained at five
160 different stations along the 3 km cross-shore transect (Fig. 1) on 24 July, 2008. Due to rapid
161 drifting when the engine was stopped before sampling, first Lagrangian station was already
162 located a 100 m away from the Eulerian station. Water depth varied little during the
163 Lagrangian survey, ranging from 40 to 70 cm. One sample was collected in the middle of the
164 water column at each station using a 1 L plastic bottle attached to a graduated stick. Short
165 wave agitation combined with limited water depth during the Lagrangian survey did not allow
166 sampling with an open-ended Nisking bottle, so a smaller closed-bottom bottle was used.
167 However, sampling bias due to accumulation of settling particles in a closed-bottom bottle
168 was reduced by a fast sampling lasting less than a few seconds and by introducing the bottle
169 upside down. Since wave length was greater than water depth, short wave agitation ensured
170 sufficient mixing over the entire water depth, making it safe to assume no stratification for all
171 sampled microorganisms (except very close to the bottom) occurred during the Lagrangian
172 survey. Each individual sample was divided into multiple aliquots to perform replicate counts.
173 Immediately before preparation of aliquots, each sample was gently agitated and subsampling
174 was performed very quickly to prevent sedimentation.

175 The Eulerian survey consisted of sampling the water column with horizontal 3 L Niskin
176 bottles at the same subtidal spot during the rising tide, starting at low tide (Fig. 1). Water
177 depth at the sampling station increased from 1.10 m at the beginning of the survey to 3.1 m at
178 the end of sampling. Three water samples were taken 0.5 m below the surface and 0.5 m
179 above the bottom of the water column during the first 2 h 45 min of the rising tide on 24 July,
180 2008. Aliquots of each sample were prepared as described above.

181

182 Mean and standard deviation of all variables at the beginning of the rising tide were
183 computed from the three samples taken at time zero of the Eulerian and Lagrangian surveys.

An 80% confidence interval for this initial measurement was computed using a Student law ($t_{n-1}(1-\alpha)=1.886$, $\alpha=10\%$). Evolution of the concentration of particulate inorganic matter (PIM) and each microorganism at the Eulerian site were predicted using on a simple mixing model based on water depth evolution, assuming that the (1) water column was well-mixed at the Eulerian site and (2) concentration of PIM or each microorganismin incoming waters could be estimated from the average concentration measured to the north of the BMO basin taken before the experiment then 15 days after. The average concentration PIM or each microorganism expected after mixing with offshore waters during tidal flow, C_t, was calculated during the Eulerian survey for sampling times after 1h15min and 2h45min as follows:

$$C_t = C_0 \frac{h_0}{h_t} + C_{ext}\left[1 - \frac{h_0}{h_t}\right]$$

where C_0 is the average concentration at time zero of the Eulerian survey, h_0 is the water depth at this time, h_t is the water depth at time t and C_{ext} is the average offshore concentration. An 80% confidence interval for this predicted value was build applying a Student law (n=3) using standard deviation of C_0 and C_{ext}. Backward trajectories reaching the Eulerian survey sampling station after 1h15min and 2h45min were also computed for the the case of no-wind tidal circulation in the BMO with the 2D barotropic model and indicated that offshore waters most probably came from the northern entrance of the BMO, west of the Charente river mouth (Fig. 1). In the absence of river flooding over the summer period, the impact of the Charente river on the pelagic ecosystem was limited at this location (Stanisière, personal communication), allowing us to assume that the concentration in the north of the BMO was spatially uniform (Ory et al. 2010). Offshore concentrations at 0.5 m below the surface were measured on July 12 and 29, 2008, at a subtidal station roughly 15 km northwest of the BMO (water depth = 17 m, 46.1153°N, 01.4139°Wr). Values for C_{ext} on July 24 were interpolated by taking the mean between offshore concentrations at the two dates (see Table 1) and

uncertainty on offshore concentrations on the day of the survey was accounted for using standard deviation between the two dates. Variability estimate based on those two days are similar to within day variability (H. Montanié, personal communication) and to within summer variability (Ory et al., 2010) in the north of BMO basin.

2.2 Physical forcings

Hydrological parameters, such as temperature and salinity, were recorded on board with multi-parameter probes (YSI 6600EDS-M) during the Eulerian survey. Average wind speed and direction were measured every hour by Météo-France at the La Rochelle Aérodrome meteorological station (46.1733°N, 1.1883°W, roughly 20 km north of the BMO). A single-point Nortek acoustic Doppler velocimeter (ADV) was used to measure the 3D velocity at 15.6 cm a.b. (above bottom, outside the wave boundary layer which thickness yielded 3 cm at maximum, Fredsoe and Deigaard,1992) and pressure as soon as the tide level was higher than 50 cm at the location 45.9161°N, 1.0890° W (Fig. 1). Thus, ADV data collection was interrupted during low tide from 12:45 h to 18:15 h on 24 July, 2008. Measurements consisted of 2 min 30 s time series recorded at a frequency of 32 Hz every 15 min for the three velocity components and pressure. Turbulent Reynolds shear stress outside the wave boundary layer were computed as the covariance of horizontal and vertical velocity deviations from the mean flow after removing wave-induced velocities. Wave-induced velocities were computed by applying a 0.5 Hz low pass filtering on raw velocity measurements (Guizien et al. 2010). Assuming a logarithmic boundary layer, bed shear stress associated with tidal current was then linearly extrapolated to the bed using Reynolds shear stress measured at 15.6 cm a.b. and zero Reynolds shear stress at the free surface.

Wave density spectra were computed from pressure time series sampled at 4 Hz and used to derive the wave parameters (i.e. mean spectral period, T_m, and significant height, H_s) over the Brouage mudflat. Assuming that the wave field was uniform over the mudflat, wave

orbital velocities at 40 cm a.b. were derived from T_m and H_s, according to the linear wave theory for varying water depths, D, at the Eulerian survey site and for a constant water depth of 40 cm during the Lagrangian survey. Time-dependent bed shear stress associated with a sine wave with these orbital velocities are described by their maximum value and average value over a wave period (half the maximum value) using Guizien and Temperville (1999) parameterization. Bed roughness was assumed to be 0.5 cm based on the bioroughness height, which could be visually estimated on the mudflat. By definition, bed friction velocity (u^*) either due to waves or to the tidal current is the square root of the bed shear stress divided by seawater density.

2.3 Particulate inorganic matter (PIM)

Total particulate matter was measured as previously described by Aminot and Chaussepied (1983). Filters were combusted at 490°C for 2 h to eliminate organic carbon content and then weighed. A water sample (from 300 to 1000 mL) was filtered onto a Whatman GF/C (47 mm in diameter) under <10 mm Hg vacuum pressure. After sample filtration, each filter was rinsed twice with MilliQ water to remove salt, dried at 60°C for 12 h then weighed to measure total particulate matter. Filters were combusted at 490°C for 2 h to eliminate organic carbon content and then weighed to determine content of particulate inorganic matter (PIM).

2.4 Enumeration of microorganisms

Water samples (up to 50 mL) were stained with 1% alkaline Lugol's solution to visualise microplanktonic cells, such as diatoms, dinoflagellates and ciliates, ranging from 20 to 200 µm. Microphytoplanktonic cells were counted using an Utermöhl settling chamber (Hydro-Bios® combined plate chambers) under an inverted microscope. Taxonomic determination was carried out in accordance with systematics literature (Nezan, 1996; Ricard,

1987; Sournia, 1986), and benthic species were differentiated from planktonic species based on knowledge of the habitat.

For nanoplanktonic cells (3 to 15 µm), water samples (up to 20 mL) were fixed using 1% paraformaldehyde then stained with DAPI (4',6'-diamidino-2-phénylindole). Autotrophic nanoflagellates (ANF) and heterotrophic nanoflagellates (HNF) were counted as previously described byby Dupuy et al. (1999), which was a modified methodology from Haas (1982), Caron (1986), and Sherr et al. (1994).

For picoeukaryotes (or picophytoeukaryotes) and *Synechococcus* (1 to 2 µm), water samples (3 mL) were fixed using 2% formaldehyde, frozen in liquid N_2, and counted using a FACSCan flow cytometer (Bd-Bioscience) as previously described by Marie et al. 2000.

For viruses (20 nm), triplicate water samples (3 mL) were fixed in filtered 2% formaldehyde and stored for less than a day at 4°C. Samples were then filtered through 0.02 µm Anodiscs (25 mm, Whatman) and counted using epifluorescence microscopy after staining for 30 min with Sybr Green I (Noble and Fuhrman, 1998). Viruses were counted in at least 15 random fields of view under blue excitation (Zeiss Axioskop 1000x). Only free viruses were enumerated.

For bacteria (1 to 2 µm), triplicate water samples (3 mL) were fixed with filtered 2% formaldehyde and stored for less than a day at 4°C. Samples were filtered through 0.02 µm Anodiscs (25mm, Whatman). Samples were enumerated using epifluorescence microscopy after staining for 30 min with Sybr Green I (Noble and Fuhrman 1998). Bacteria were counted in at least 15 random fields of view under blue excitation (Zeiss Axioskop 1000x). Free bacteria were counted with a fixed focalisation on the filter surface while attached bacteria on aggregates deposited on the filter were screened by varying focal distance.

For each group of autotrophic or heterotrophic organisms, biomass was calculated using conversion factor for cell to carbon content (Table 2) multiplied by abundance.

3. Results

3.1 Physical forcings

On 24 July, a thermal wind in the morning turned from the southeast (land) to the west (sea), reaching a maximum speed of 8.7 m s^{-1} around low tide at 15:00 h (Fig. 3a). Short period waves, with a mean period ranging from 2 to 4 s, started growing under wind action after 11:00 h during ebb tide. At 12:30 h, when the ADV emerged, significant wave height was already 0.15 m and had increased up to 0.2 m at 18:30 h when ADV was submerged again at the end of the rising tide (Fig. 3a). Given the slight decrease in wind speed after 15:00 h and based on personal observation, wave height was at least 0.2 m during the survey period from 15:45 h to 18:30 h. Therefore, a wave height of 0.2 m was used to estimate bed friction velocity caused by waves. Maximum and mean bed friction velocity due to waves were at least 4.5 cm s^{-1} and 3.2 cm s^{-1}, respectively, during the Lagrangian survey under 0.4 m water depth. In contrast, maximum and mean bed friction velocities due to waves were less than 2 cm s^{-1} and 1.4 cm s^{-1}, respectively, when the Eulerian survey started at low tide. These values continuously decreased to 0.5 cm s^{-1} and 0.35 cm s^{-1}, respectively, as the water level rose (Fig. 3b). Bed friction velocity induced by the tidal current reached a maximum value of 1.3 cm s^{-1} when the tidal flow arrived at the ADV location (water depth of 0.5 m) and rapidly decreased to less than 0.5 cm s^{-1} during the rest of the rising tide over the intertidal mudflat.

3.2 Changes in the concentration of particulate inorganic matter during the Eulerian and Lagrangian surveys

PIM concentration displayed a large spatial variability at the beginning of the rising tide surveys (Fig. 4), with a value that was twice as high in the subtidal site (300 mg L^{-1}) compared to the first Lagrangian sampling station (140 mg L^{-1}). However, at the end of the Lagrangian survey, the PIM concentration had increased more than five-fold, up to 1180 mg L^{-1}, largely overpassing the 80% confidence interval around the initial average concentration.

313 Moreover, PIM concentration steadily increased at an average rate of 0.11 mg L^{-1} s^{-1} as tidal
314 flow progressed over the mudflat (Fig. 4). Meanwhile, the rate of increase in the PIM
315 concentration was not constant throughout the survey, reaching 0.18 mg L^{-1} s^{-1} during the first
316 hour, falling to 0.02 mg L^{-1} s^{-1} during the next 40 min and again increasing to 0.12 mg L^{-1} s^{-1}
317 for 30 min before falling again to 0.05 mg L^{-1} s^{-1} during the last 30 min. Assuming a uniform
318 vertical PIM concentration over the 0.4 m water depth due to strong wave agitation, erosion
319 rates decreased from 460 mg m^{-2} s^{-1} in the lower part of the mudflat during the first hour to 60
320 mg m^{-2} s^{-1} in the middle part of the mudflat during the next 40 min and increased again to 300
321 mg m^{-2} s^{-1} during the next 30 min. In contrast, in the Eulerian survey, PIM concentration
322 decreased, with values remaining within the 80% confidence interval of predicted dilution by
323 offshore waters (Fig. 4).
324
325 *3.3 Changes in the concentration of autotrophic microorganisms during the Eulerian*
326 *and Lagrangian surveys*
327 The dynamics of the various taxa of autotrophic microorganisms counted during the
328 Lagrangian and Eulerian surveys was compared to initial concentration and predicted changes
329 by mixing with offshore waters, respectively. At the beginning of both surveys, two third of
330 diatoms were benthic species. This proportion increased during the Lagrangian survey to
331 nearly 80%. In the Eulerian survey, this proportion decreased to less than 20%, reflecting the
332 differential effect of resuspension and mixing with offshore waters on water column
333 microorganism dynamics. Although changes in benthic diatom concentration during the
334 Lagrangian survey suggested alternate phases of gain in the lower and upper parts of the
335 mudflat, where erosion was the greatest, and loss in the middle regions of the mudflat, none of
336 these changes were beyond the 80% confidence interval of the initial concentrations
337 determined at the beginning of the survey (Fig. 5a). However, the decrease in benthic diatom
338 concentration was not statistically significant. In contrast, a predicted significant increase in

pelagic diatoms was observed during the Eulerian survey. During the Lagrangian survey, changes in pelagic diatoms concentration were again not statistically significant given the large variability observed at the beginning of survey (Fig. 5b).

Smallest autotrophs were mainly comprised of ANF (0.6 to 1 x 10^4 cells mL^{-1}) in both surveys, whereas picophytoeukaryotes and *Synechococcus* sp. (e.g. cyanobacteria) displayed very low concentrations (Fig. 5b-d). During the Lagrangian survey, ANF concentration nearly doubled during the first 1h15 min, departing from 80% confidence interval around value when surveys started, and then decreased during the next hour (Fig. 5b). During the Eulerian survey, ANF concentration displayed opposite dynamics at the surface and at the bottom. In any case, by the end of the survey, values at the surface and at the bottom overpassed the 80% confidence interval around values predicted from dilution with offshore waters.

Picoeukaryotes concentration steadily decreased during the Lagrangian survey. However, this trend was not statistically significant given the large variation coefficient at the beginning of survey (Fig. 5c). During the Eulerian survey, picoeukaryote concentration displayed opposite dynamics at the surface and at the bottom, increasing at the surface and decreasing at the bottom (Fig. 5c). However, values were never outside the large 80% confidence interval around values predicted from mixing with offshore waters.

The concentration of *Synechococcus* sp. remained fairly constant (4.5 x 10^3 cells mL^{-1}) during both surveys (Fig. 5d), with values lower than the 80% confidence interval of predicted mixing by offshore waters.

3.4 *Changes in the concentration of heterotrophic microorganisms during the Eulerian and Lagrangian surveys*

During the Lagrangian survey, free virus concentration steadily decreased from 1.2 x 10^7 particles mL^{-1} to 7 x 10^6 particles mL^{-1} (Fig. 6a). However, this decrease was not statistically significant. During the Eulerian survey, free virus concentration at the surface

steadily decreased within the 80% confidence interval of predicted dilution by offshore waters. Conversely, at the bottom, free virus concentration significantly increased during the first 1h15 min, reaching a value of 1.8 x 10^7 viruses mL^{-1}. This value was out of the 80% confidence interval around values predicted from dilution by offshore waters and even out of the 80% confidence interval around value when survey started. However, free viruse concentration at the bottom decreased during the next 1h30 min, reaching a value of 4 x 10^6 viruses mL^{-1}, which was within the 80% confidence interval around values predicted from dilution by offshore waters.

Free bacteria dynamics were similar to free virus dynamics during both surveys (Fig. 6b). For attached bacteria concentration, no significant change was observed during the Lagrangian survey (6–8 x 10^6 cells mL^{-1}), while concentration decreased during the Eulerian survey by one order of magnitude, which was still within the 80% confidence interval of predicted dilution with offshore waters (Fig. 6c).

The dynamics of HNF was similar to the ANF dynamics in the both surveys. During the Lagrangian survey, HNF concentration increased steadily over the first 2 h10 min to almost twice the concentration measured at the start of the survey (3 x 10^3 cells mL^{-1}), but then decreased during the last 30 min (Fig. 6d). During the Eulerian survey, HNF concentration displayed opposite dynamics at the bottom and at the surface, but both values remained within the 80% confidence interval around surveys initial value and the large 80% confidence interval around values predicted from mixing with offshore waters (1.3 x 10^3 cells mL^{-1}).

During the Lagrangian survey, ciliate concentration doubled along the transect to values greater than the 80% confidence interval estimated when the survey began (Fig. 6e). During the Eulerian survey, ciliate concentration decreased at the bottom and at the surface more than expected from dilution with offshore waters at the bottom (i.e. lower than the 80% confidence interval).

In summary, the water column only became significantly enriched with nanoflagellates (autotrophs and heterotrophs) and ciliates during the Lagrangian survey over the mudflat, where resuspension occurred. In contrast, mixing (typically leading to dilution) with offshore waters was observed at the Eulerian site, except for free viruses and free bacteria at the bottom (gain), ANF (gain) and *Synechococcus* and ciliates (loss). No significant change was detected in autotroph biomass in any of the surveys (Fig. 7a) or in heterotroph biomass during the Lagrangian survey (Fig. 7b). In contrast, heterotroph biomass was decreased by 50% at the end of the Eulerian survey as expected from dilution with less heterotrophic offshore waters (Fig. 7b). Regardless, heterotroph biomass remained greater than autotroph biomass throughout both surveys.

4. Discussion

In the present study, we aimed at testing in situ whether and how the pelagic system structure was modified during the rising tide by physical transfer of autotrophic and heterotrophic microorganisms. Physical transfer included mixing with offshore waters and sediment erosion and was evidenced by temporal changes in particulate inorganic matter concentration.

4.1 Decrease of resuspended microorganisms by grazing predators

Over the mudflat, significant sediment erosion occurred under wave action, but at different rates across the intertidal area. These changes were reflected by subsequent changes in erodibility across the mudflat as bed friction velocity was kept constant during the Lagrangian survey. A very low erosion rate in the middle region of the Brouage mudflat with large bed friction velocities was indicative of low erodibility of the consolidated sediment, possibly due to desiccation during tidal emersion (Anderson and Howell 1984; Paterson et al. 1990). On July 24, water content in the upper layer of mud fell from 55 to 46% during the 4 h low tide. Such periods of desiccation occurred on many days throughout the particularly dry,

windy and hot month of July 2008 (Dupuy et al., personal communication). Variability in erosion rates across the mudflat may also be attributed to changes in bioturbation intensity (Widdows et al. 1998). Specifically, more active bioturbators in the Brouage mudflat, such as *Scorbicularia plana (*Orvain 2005), are generally more abundant in the upper mudflat (Sauriau et al. 1989; Bocher et al. 2007; Orvain et al. 2007). Moreover, erodibility increase due to bioturbation activity should also be enhanced by low tide duration: the upper in the mudflat, the longer the low tide and hence, the higher the bioturbation pressure. Surprisingly, the input of taxon that are generally abundant in the sediment, such as diatoms, bacteria and nanoflagellates (Paterson et al. 2009), was not observed during sediment erosion. Differences in resuspension thresholds for benthic microorganisms may have been due to cell size, specific gravity, behaviour, or association with particles (Shimeta et al. 2002). However, bed friction velocities reaching an average of 3.2 cm s^{-1} due to waves prevented sedimentation of particles with settling velocities less than 4 cm s^{-1} (i.e. particles with diameters smaller than 320 µm) (Fredsöe and Deigaard 1992). Thus, considering the much lower density of organic matter compared to sedimentary matter and suspension thresholds determined by Shimeta et al. (2002), suspension thresholds were reached for all microorganisms included in the present study. Moreover, wave vertical velocities were undoubtedly greater than the swimming speed of any of these microorganisms (<1 mm s^{-1}, Bauerfeind et al. 1986), precluding any migration process. In addition, all microorganisms counted in the present study were found at high densities in the Brouage muddy sediment before the rising tide, except for ciliates. As such, a significant increase in microorganism concentrations was expected to occur along with erosion of the muddy bed. Conversely, a stagnation or a decrease in the concentration of any microorganism during the Lagrangian survey therefore most likely indicated consumption by grazers.

Guarini et al. (2008) developed a model that simulates the dynamics of microalgal biomass in semi-enclosed littoral ecosystems and suggested that resuspension of the MPB

443 occurs at the beginning of the rising tide, even in the absence of simultaneous sediment
444 erosion. Such recurrent MPB resuspension is consistent with the high proportion of benthic
445 diatom species observed at the beginning of both surveys in the present study. Meanwhile,
446 enrichment in benthic diatoms species was not significant in our survey. However, benthic
447 diatom concentration simultaneously increased with mud erosion in the lower and upper part
448 of the mudflat. Of the smaller autotrophs, only ANF significantly increased in the lower part
449 of the mudflat, where sediment erosion was greatest, during the first hour of the Lagrangian
450 survey. This significant increase in ANF concentration in the water column suggests that ANF
451 concentrations in eroded sediment during the survey was at least 10^6 cell mL^{-1}, which is a
452 hundred times greater than previously reported average values in the first top cm of the BMO
453 sediment (10^4 cell mL^{-1}, C. Dupuy personal communication). Yet, ANF most probably
454 accumulated at the very surface of sediment in a layer of 1-2 cells thickness, just like diatoms
455 does, to photosynthesize (Guarini et al., 2000). These findings support routine measurement
456 of the detailed vertical distribution of microorganisms for estimation of erosion fluxes.
457 *Synechococcus* concentrations remained low, and picophytoeukaryote concentration
458 decreased during the same period. We therefore suggest that the erosion flux of benthic
459 diatoms and ANF, largely present at the mud surface, was immediately overwhelmed by a
460 grazing flux due to heterotrophic protists (HNF, ciliates), micrometazoan and mesometazoans
461 planktonic organisms (Sherr et al. 1986; Leakey et al. 1992; Calbet et al. 2008) or benthic
462 suspension feeders (Hughes 1969; Carlson et al. 1984).

463 Free virus concentration decreased during the Lagrangian survey, while it was expected
464 to increase with resuspension as these microorganisms are also largely present in mud (10^{10}
465 cell mL^{-1} sediment; Hewson et al. 2001, and the present study). Again, this suggests that virus
466 resuspension flux during the rising tide due to waves was compensated by a loss process.
467 However, adsorption of free viruses onto clay particles may also occur in addition to or as an
468 alternative to grazing (Malits and Weinbauer 2009). Reversible sorption and hydrophobic

effects are linked to the ionic strength of the given environment, most notably to the concentration of cations like Na^+ , which may change between bed sediment and water (Gerba 1984). Finally, water agitation has been recently shown to enhance viral sorption to clay (Syngouna and Chrysikopoulos 2010). Therefore, together with wave agitation, availability of sorption sites on the clayed mud of the BMO (Helton et al. 2006), salt water may favour virus adsorption onto sedimentary particles. Similar to viruses, electrostatic properties, pH, temperature, and salinity are thought to govern the sorption of bacterial cells onto clay minerals (Jiang et al. 2007). As such, bacteria adsorption onto resuspended sedimentary particles should not be excluded during the Lagrangian survey. Free bacteria concentration remained constant while an increase was expected as these organisms are abundant in the mud (5.10^8 cell mL^{-1}, Garet 1996 and 10^9 cell mL^{-1} in the present study) and were undoubtfully resuspended. However, no significant enrichment in attached bacteria was observed during the Lagrangian survey despite that a thousand-fold enrichment was expected from the large PIM increase (ten-fold) and the high concentration of bacteria in bed sediment (10^9 cell mL^{-1}) compared to water (10^6 cell mL^{-1}). As free virus concentration did not strongly increased, significant enhancement of virally mediated bacterial mortality was unlikely. Thus, attached and free bacteria were most likely heavily grazed immediately after resuspension during the Lagrangian survey.

Significant HNF concentration increase during the Lagrangian survey is consistent with expected resuspension of benthic HNF given the bed friction velocities (due to waves) that largely exceeded thresholds for HNF resuspension (Shimeta et al. 2002; 0.25-0.80 cm s^{-1}). In contrast, HNF production (secondary production) could not explain concentration doubling, given nanoplankton growth rate ranging from 7 h (Dupuy et al, 2007) to 20 h (Calbet et al. 2008; Liu et al. 2009). Thus, doubling of HNF concentration in the water column suggest that HNF concentration in eroded sediment during the survey was roughly 10^5 cell mL^{-1}, which is a hundred times greater than previously reported average values found in the first top cm of

the BMO sediment (10^3 cell mL^{-1}, C. Dupuy personal communication). This result suggests that HNF accumulated at the very surface of sediment during the present study and pinpoints again the importance of accounting for vertical distribution of microorganisms when estimating erosion fluxes. Similar zonation of nanoflagellates at the surface of sediment compared to deeper layers have been previously reported during summer periods in the North Sea (Hondeveld et al. 1994) and also in the BMO in July 2008 (Dupuy et al., submitted). In any case, after 2 h, the decrease in HNF concentration during the Lagrangian survey indicated grazing on HNF by ciliates or micrometazoan and mesometazoan planktonic organisms (Sherr et al. 1986; Hartmann et al. 1993; Calbet et al. 2008) also buffered resuspension flux.

In contrast, a significant increase in ciliate concentration during the Lagrangian survey could not be attributed to benthic transfer that accompanies mud erosion. Although some ciliate genera can be found in sediment, such as scuticociliates (*Uronema* sp.), ciliate concentration is generally very low in mud sediments (Giere 1993), with concentrations lower than 20 cell mL^{-1} in the BMO surficial sediment (C. Dupuy, personal communication). Simulated erosion of sediment cores taken in the BMO during the same period as the present study confirmed ciliates erosion was unsignificant (C. Dupuy, personal communication). Besides, ciliates taxa found in the present study were Order Oligotrichida (*Strombidium* spp.) and Order Tintinnida (*Tintinnopsis* spp.), which are generally part of the suprabenthos due to behavioural adaptations leading to depth zonation above the sediment-water interface after vertical migration when vertical flow motion is small. Compared to other groups of microorganisms analysed in the present study, ciliates are relatively more motile organisms (velocities up to 0.5 mm s^{-1}) that can control their position in the water column at low turbulence levels (Jonsson 1989). Ciliate concentration increase during the Lagrangian survey may be attributed to redistribution by waves vertical stirring of ciliates accumulated at a particular depth during slack tide.

4.2 Mixing with offshore waters

Mixing (dilution or enrichment) with offshore waters was expected during the Eulerian survey, where water depth varied. It should be noted that the 80% confidence interval around prediction from mixing with offshore waters reduces when offshore waters are less concentrated than inner basin waters (heterotrophic microorganisms) while it is reversed when offshore are more concentrated than inner basin waters (autotrophic microorganisms). Thus, detecting deviation from dilution prediction should be more accuratethan detecting deviation from import prediction.

The PIM concentration evolved as predicted by dilution during the Eulerian survey, indicating that no significant erosion or sedimentation occurred. Thus, settling velocity of suspended particles should be comparable to mean wave bed friction velocities, ranging from 1.4 to 0.5 cm s^{-1}, while bed sediment erosion threshold should be larger than 1.4 cm s^{-1}. In contrast, during the Lagrangian survey, a strong increase in PIM concentration indicated that bed friction velocities were high enough to erode the mud. Bed friction velocity due to the tidal current (1.3 cm s^{-1}) was lower than the largest bed friction velocity observed during the Eulerian survey which did not cause significant erosion. Thus, mud erosion during the Lagrangian survey was more likely driven by bed friction velocities due to waves (average velocity of 3.2 cm s^{-1} and 4.5 cm s^{-1} maximum) as suggested by Bassoullet et al. (2000). However, the current study only indicates that the erosion threshold for the fine-grained mud sediment of the Brouage mudflat (median grain size was 10 to 12 µm) lies between 1.4 cm s^{-1} (largest value during Eulerian survey during which erosion was not observed) and 4.5 cm s^{-1} (largest value during Lagrangian survey during which erosion was obsrved) in terms of bed friction velocity.

During the Eulerian survey, no significant change in diatom concentration was detected reflecting similar order of magnitude of concentration in the inner basin and in the north of

547 the basin. However, a total community change occurred with replacement of benthic diatoms
548 by pelagic diatoms in proportion of water depth change during the rising tide. No significant
549 primary production of diatoms was expected given the short duration of the Eulerian survey
550 compared to the generation time for microphytoplankton (1 division d^{-1}, Calbet and Landry
551 2004 to 2 divisions d^{-1}, Dupuy et al. 2007) and water turbidity (Struski and Bacher 2006;
552 Bouman et al. 2010). Thus, mixing was the most likely dominant process.

553 Significantly lower than expected concentrations (based on mixing with offshore
554 waters) of low motility *Synechococcus* (at the surface and at the bottom) suggest that grazing
555 pressure was strong during tidal flow due to microzooplankton, mesozooplankton and/or
556 bivalve mollusks (*Macoma balthica*, *Scrobicularia plana*) (Hugues 1969; Hartmann et al.
557 1993; Dupuy et al. 1999). Ciliates also exhibited lower than expected concentrations at the
558 bottom. However, for these motile organisms, the assumption of a vertically homogeneous
559 distribution was probably no longer true as turbulence intensity decayed during the Eulerian
560 survey. Thus, ciliates losses may not be attributed to grazing only. Motility may also explain
561 the opposite dynamics of nanoflagellates during the Eulerian survey between surface and
562 bottom, given their swimming speed can reach 0.3 to 0.5 mm s^{-1} and yield a transport of 1 to 2
563 m after one hour (Bauerfeind et al. 1986). However, an overall significant increase in ANF
564 concentration at the end of the Eulerian survey suggested that primary production started.

565 Conversely, during the first portion of the Eulerian survey, free virus and free bacteria
566 concentration significantly increased at the surface compared to the offshore water dilution
567 curve, suggesting that secondary production or desorption dominated over grazing. This
568 synchronous increase was congruent with the synchronous virus and bacteria dynamics
569 usually observed in BMO at the monthly scale in summer (Ory et al. 2010, 2011).

570

571 *4.3 Strengths and limitations of the sampling strategy*

Adapting sampling strategy to disentangle mixing with offshore waters and resuspension and separating physical processes from biotic processes using PIM as a reference lead to the conclusion that grazing pressure must be intense during rising tide. However, temporal changes in concentrations that follow the dilution curve in an Eulerian survey or remain constant in a Lagrangian survey simply mean that loss and gain processes balance each other out. In addition, conclusive demonstration of loss or gain processes requires that temporal changes in surveys are larger than uncertainties on initial conditions. In the present study, uncertainties in PIM, diatoms, picoeukaryotes and attached bacteria concentrations at the beginning of surveys reached 100%, which prevented the detection of any significant decrease. Yet, significant increases could be detected when values more than doubled, as seen for PIM. These large uncertainties have different origins. For PIM, uncertainties were mainly due to large differences between the Lagrangian and Eulerian samples taken when surveys started and advocate for increasing sampling effort and localization precision in the intertidal area where large horizontal spatial gradients may exist. For diatoms, attached bacteria and picoeukaryotes, large uncertainties also came from large difference between the Eulerian samples and points out the low precision on concentration determination for some microorganisms. Reducing these uncertainties requires increased sample volume and superior enumeration efforts.

5. Conclusions

During a rising tide, expected water column enrichment of benthic microorganisms (small to large autotrophs and heterotrophs) from sediment resuspension was largely overwhelmed by loss processes, except for nanoflagellates (ANF and HNF). The dominant loss process was likely grazing. However, adsorption onto clayed particles may have also masked enrichment for free viruses and bacteria . A combination of resuspension and grazing/adsorption processes led to non-significant changes in both heterotroph and autotroph

598 total biomass during the rising tide in the nearshore area. In the meanwhile, offshore waters
599 imported autotrophic organisms, mainly *Synechococcus*, while heterotrophic microorganisms
600 were diluted. However, autotrophic organisms import was significantly grazed. As a result,
601 combination of offshore waters import and grazing led to stability of autotrophs biomass in
602 the deeper areas of the BMO, while heterotrophs biomass was reduced by 50%. Lastly, when
603 resuspension occurred over a tidal flat during a rising tide, the water column evolved to a less
604 heterotrophic structure over the mudflat in the deepest part of the semi-enclosed bay
605 compared to nearshore. Thus, the present study suggests that this differential evolution mainly
606 reflects dilution with low concentrated offshore waters, as grazing pressure erased any
607 microorganisms inputs accompanying physical transfers due to bed erosion or offshore waters
608 mixing.
609
610 **Acknowledgments**
611 The work was supported by the French ANR (Agence Nationale pour la Recherche)
612 through the VASIREMI project “Trophic significance of microbial biofilms in tidal flats”
613 (grant no. ANR-06-BLAN-0393-01). We are grateful to Martine Bréret, Camille Fontaine,
614 Françoise Mornet and the personnel at both RV Tidalou and Estran for their technical support.
615 We thank Pierre Richard for the Lagrangian buoys. We are also grateful to Carolyn Engel-
616 Gautier and Proof-reading-service.com Ltd for English corrections.
617
618
619
620
621
622
623

References

Alongi, D. M. 1991. Flagellates of benthic communities: characteristics and methods of study, p. 57–75. In D. J. Patterson [ed.], The Biology of Free-living Heterotrophic Flagellates. Clarendon Press, Oxford.

Aminot, A., and M. Chaussepied. 1983. Manuel des analyses chimiques en milieu marin. CNEXO, Brest.

Anderson, F. E., and B. A. Howell. 1984. Dewatering of an unvegetated muddy tidal flat during exposure – dessication or drainage? Estuaries **7**: 225–232.

Bassoulet, P., P. Le Hir, D. Gouleau, and S. Robert. 2000. Sediment transport over an intertidal mudflat: field investigations and estimation of fluxes within the `Baie de Marennes-Oleron (France). Cont. Shelf Res. **20**: 1635–1653.

Bauerfeind, E., Elbrächter, M., Steiner, R. and J. Thronden. 1986. Application of Laser Doppler Spectroscopy (LDS) in determining swimming velocities of motile phytoplankton. Mar Biol **93**: 323-327.

Blanchard, G.F, and V. Cariou-Le Gall. 1994. Photosynthetic characteristics of microphytobenthos in Marennes-Oleron Bay, France : Preliminary results. J. Exp. Mar. Biol. Ecol. **182**: 1–14.

Blanchard, G.F., J. M. Guarini, P. Richard, and P. Gros. 1997. Seasonal effect on the relationship between the photosynthetic capacity of intertidal microphytobenthos and short-term temperature changes. J. Phycol. **33**: 723–728.

Blanchot, J., and M. Rodier. 1996. Picophytoplankton abundance and biomass in the western tropical Pacific Ocean during the 1992 El Nino year: results from flow cytometry. Deep Sea Res Part I: Oceanogr. Res. Papers **43**: 877–895.

Bocher, P., T. Piersma, A. Dekinga, C. Kraan, M. G. Yates, T. Guyot, E. O. Folmer, and G. Radenac. 2007. Site- and species-specific distribution patterns of mollusks at five

intertidal soft-sediment areas in northwest Europe during a single winter. Mar. Biol. **151**:577–594.

Bouman, H. A. , T. Nakane, K. Oka, K. Nakata, K. Kurita, S. Sathyendranath, and T. Platt. 2010. Environmental controls on phytoplankton production in coastal ecosystems: A case study from Tokyo Bay. Est. Coast. Shelf. Sci. **87**: 63–72.

Calbet, A., and M. R. Landry. 2004. Phytoplankton growth, microzooplankton grazing, and carbon cycling in marine systems. Limnol. Oceanogr. **49**:51–57.

Calbet, A., I. Trepat, R. Almeda, V. Saló, E. Saiz, J. I. Movilla, M. Alcaraz, L. Yebra, and R. Simó. 2008. Impact of micro- and nanograzers on phytoplankton assessed by standard and size-fractionated dilution grazing experiments. Aquat. Microb. Ecol. **50**: 145–156.

Cammen, L.M. 1991. Annual bacterial production in relation to benthic microalgal production and sediment oxygen uptake in an intertidal sandflat and an intertidal mudflat. Mar. Ecol. Prog. Ser.**71**: 13–25.

Caron, D. A. 1983. Technique for enumeration of heterotrophic and phototrophic nanoplankton, using epifluorescence microscopy, and comparison with other procedures. Appl. Environ. Microbiol. **46**: 491–498.

Carlson, D.Townsend, D. W., Hilyard, A. L., Eaton J. F. 1984. Effect of an Intertidal Mudflat on Plankton of the Overlying Water column. Can. J. Fish. Aquat. Sci., 41, 1523-1528.

Danovaro, R., C. Corinadelsi, M. Filippini, U. R. Fisher, M. O. Gessner, S. Jacquet, M. Magagnini, and B. Velimirov. 2008. Viriobenthos in freshwater and marine sediments: a review. Fresh. Biol. **53**: 1186–1213.

Dupuy, C., S. Le Gall, H. J. Hartmann, and M. Bréret. 1999. Retention of ciliates and flagellates by the oyster *Crassostrea gigas* in French Atlantic coastal ponds: protists as a trophic link between bacterioplankton and benthic suspension-feeders. Mar. Ecol. Prog. Ser. **177**: 165–175.

675 Dupuy, C., A. Pastoureaud, M. Ryckaert, P. G. Sauriau, and H. Montanié. 2000. Impact of the
676 oyster Crassostrea gigas on the microbial community in Atlantic coastal ponds near La
677 Rochelle. Aquat. Microb. Ecol. **22**: 227–242.
678 Dupuy, C., M. Ryckaert, S. Le Gall, and H. J. Hartmann. 2007. Seasonal variations of
679 planktonic communities in Atlantic Coastal pond: importance of nanoflagellates.
680 Microb. Ecol. **53**: 537–548.
681 Epstein, S. S. 1997. Microbial food webs in marine sediments. I. Trophic interactions and
682 grazing rates in two tidal flat communities. Microb. Ecol. **34**:188–198.
683 Fenchel, T. 1969. The ecology of marine microbenthos. IV. Structure and function of the
684 benthic ecosystem, its chemical and physical factors and the microfauna communities
685 with special reference to the ciliated protozoa. Ophelia **5**:1–182.
686 Fredsoe, J., and R. Deigaard. 1992. Mechanics of coastal sediment transport. 369 p. In World
687 Scientific [ed.], Advanced Series on Ocean Engineering 3.
688 French, J.R., H. Burningham, and T. Benson. 2008. Tidal and Meteorological Forcing of
689 Suspended Sediment Flux in a Muddy Mesotidal Estuary. Estuaries Coasts **31** : 843–
690 859.
691 Fournier, J., Dupuy, C., Bouvy, B., Courrodon-Real, M., Charpy, L., Pouvreau, S., Le
692 Moullac, G., Le Pennec, M., Cochard, J.C. 2012 Pearl oysters *Pinctada margaritifera*
693 grazing on natural plankton in Ahe atoll lagoon (Tuamotu archipelago, French
694 Polynesia). Marine Pollution Bulletin **65** : 490–499
695 Garet, M. J. 1996. Transformation bactérienne de la matière organique dans les sédiments
696 côtiers. Relation entre les métabolismes respiratoires et les activités exoprotéolytiques
697 bactériennes, phD Microbiologie : Univ. Bordeaux 2.
698 Garstecki, T., S. A. Wickham, and H. Arndt. 2002. Effects of experimental sediment resus-
699 pension on a coastal planktonic microbial food web. Est. Coast. Shelf. Sci. **55:** 751–762.

Gasol, J. M. 1993. Benthic flagellates and ciliates in fine freshwater sediments: calibration of a live counting procedure and estimation of their abundances. Microb. Ecol. **25**:247–262.

Gerba, C. P. 1984. Applied and theoretical aspects of virus adsorption to surfaces, 30: 133-168. In Advances in Applied microbiology [ed.], Academic press, Inc.

Giere, O. 1993. Meiobenthology. The microscopic fauna in aquatic sediments, 328 pp. Springer-Verlag, Berlin.

Grémare, A., Amouroux, J.M., Cauwet, G., Charles, F., Courties, C., deBovée, F., Dinet, A., Devenon, J.L., Durrieu de Madron, X., Ferré, B., Fraunié, P., Joux, F., Lantoine, F., Lebaron, P., Naudin, J.J., Palanques, A., Pujo-Pay, M., Zudaire, L. 2003. The effects of a strong winter storm on physical and biological variables at a shelf site in the Mediterranean. Oceanologica Acta, 26(4), 407-419.

Guarini, J. M., Blanchard, G.F., Gros, Ph., Gouleau, D., Bacher, C. 2000. Dynamic model of the short-term variability of microphytobenthic biomass on temperate intertidal mudflats. Mar. Ecol. Prog. Ser. **195**: 291-303.

Guarini, J. M., N. Sari, and C. Moritz. 2008. Modelling the dynamics of the microalgal biomass in semi-enclosed shallow-water ecosystems. Ecol. Modeling **211**: 267–278.

Guizien, K., F. Charles, D. Hurther, and H. Michallet. 2010. Spatial redistribution of *Ditrupa arietina* (soft bottom Mediterranean epifauna) during a moderate swell event: evidence and implications for biotic quality indices. Cont. Shelf Res. **30**: 239–251.

Guizien, K., and A. Temperville. 1999. Frottement de fond sous une houle irrégulière. C. R. Acad. Sci. Paris, t. 327, Série Iib: 1375–1378.

Haas, L.W. 1982. Improved epifluorescence microscopy for observing planktonic microorganisms. Ann. Inst. Oceanogr. **58**: 261–266.

724 Hartmann, H. J., H. Taleb, L. Aleya, and N. Lair. 1993. Predation on ciliates by the
725 suspension-feeding calanoid copepod *Acanthodiaptornus denticornis*. Can. J. Fish.
726 Aquat. Sci. Paris. **50**:1382–1393.
727 Hervouet, J. M., and L. Van Haren. 1994. TELEMAC-2D Principle Note (Electricité de
728 France, Technical Report HE- 43/94/051/B).
729 Hervouet, J. M. 2007. Hydrodynamics of Free Surface Flows: Modelling With the Finite
730 Element Method, Wiley-Blackwell, 360 pp.
731 Hewson, I., J. M. O'Neil, C. Heil, G. Bratbak, and D. Dennison. 2001. Effects of concentrated
732 viral communities on photosynthesis and community composition of co-occuring
733 benthic microalgae and phytoplankton. Aquat. Microb. Ecol. **25**: 1–10.
734 Herlory, O., J. M. Guarini, P. Richard, and J. F. Blanchard. 2004. Microstructure of
735 microphytobenthic biofilm and its spatio-temporal dynamics in an intertidal mudflat
736 (Aiguillon Bay, France). Mar. Ecol. Prog. Ser. **282**: 33–44.
737 Hondeveld B.J.M., Nieuwland G., van Duyl F.C., Bak R.P.M. 1994. Temporal and spatial
738 variations in heterotrophic nanoflagellate abundance in North Sea sediment. Mar. Ecol.
739 Prog. Ser. **109**: 235-243.
740 Hughes, R.N. 1969. A study of feeding in *Scrobicularia plana*. J. Mar. Biol. Ass. U. K. **49**:
741 805–823.
742 Jiang, D., Q. Huang, P. Cai, X. Rong, and W. Chen. 2007. Adsorption of *Pseudomonas*
743 *putida* on clay minerals and iron oxide. Colloids and surfacesB : Biointerfaces **54**: 217–
744 221.
745 Jonsson P.R. 1989. Vertical distribution of planktonic ciliates – an experimental ciliates : an
746 experimental analysis of swimming behaviour. Mar. Ecol. Prog. Ser. **52**: 39-53.
747 Kemp, P. F. 1988. Bacterivory by benthic ciliates: significance as a carbon source and impact
748 on sediment bacteria. Mar. Ecol. Prog. Ser. **49**:163–169.

749 Koroleff, F., 1969. Direct determination of ammonia as indophenol blue. International
750 Council for the Exploration of the Sea, 1969/C:9, Hydrol Commun, pp 19-22.
751 Labry, C., A. Herbland, and D. Delmas. 2002. The role of phosphorus on planktonic
752 production of the Gironde plume waters in the Bay of Biscay. J. of Plankton Res. **24**:
753 97–117.
754 Leakey, R. J. G., P. H. Burlull, and M. A. Sleigh. 1992. Planktonic ciliates in Southampton
755 Water: abundance, biomass, production, and role of pelagic carbon flow. Mar. Biol. **14**:
756 67–83.
757 Liu, H., K. Suzuki, J. Nishioka, R. Sohrin, and T. Nakatsuka. 2009. Phytoplankton growth
758 and microzooplankton grazing in the Sea of Okhotsk during late summer of 2006.
759 Deep-Sea Res. I. **56**: 561–570.
760 Lucas, C.H., J. Widdows, M. D. Brinsley, P. N. Salkeld , and P. M. J. Herman. 2000. Benthic-
761 pelagic exchange of microalgae at a tidal flat. 1. Pigment analysis. Mar. Ecol. Prog. Ser.
762 **196**: 59–73.
763 Malits, A., and M. G. Weinbauer. 2009. Effect of turbulence and viruses on prokaryotic cell
764 size, production and diversity. Aquat. Microb. Ecol. **54**: 243–254.
765 Marie, D., F. Partensky, N. Simon, L. Guillou, and D. Vaulot. 2000. Flow cytometry analysis
766 of marine picoplankton. In: Diamond RA, DeMaggio S [ed.], In living color. Protocols
767 in flow cytometry and cell sorting. Springer-Verlag, Berlin.
768 Marquis, E., N. Niquil, D. Delmas, H. J. Hartmann, D. Bonnet, F. Carlotti, A. Herbland, C.
769 Labry, B. Sautour, P. Laborde, and C. Dupuy. 2007. Planktonic food web dynamics
770 related to phytoplankton bloom development on the continental shelf of the Bay of
771 Biscay, French coast. Est. Coast. Shelf. Sci. **73**: 223–235.
772 Mehta, J.A., E. J. Hayter, W. R. Parker, R. B. Krone, and A. M. Teeter. 1989. Cohesive
773 sediment transport. I. Process description. J. Hydraulic Eng. **115**:1076–1093.

774 Nezan, E., 1996. Surveillance du Phytoplankton marin : manuel illustré adapté à la formation
775 des analystes. (IFREMER, Eds.). Brest.
776 Nicolle, A., and M. Karpytchev. 2007. Evidence for spatially variable friction from tidal
777 amplification and asymmetry in the Pertuis Breton (France). Cont. Shelf Res. **27**: 2346–
778 2356.
779 Noble, R.T., and J. A. Fuhrman. 1998. Use of SYBR Green I for rapid epifluorescence counts
780 of marine viruses and bacteria. Aquat. Microb. Ecol. **14**: 113–118.
781 Orvain, F. 2005. A model of sediment transport under the influence of bioturbation activities:
782 generalisation to a key-species Scrobicularia plana. Mar. Ecol. Progr. Ser. **286**: 43–56.
783 Orvain F., P. G. Sauriau, A. Sygut, L. Joassard, and P. Le Hir. 2004. Roles of *Hydrobia ulvae*
784 bioturbation and the physiological stage of microphytobenthic mats in resuspended
785 sediment and pigment fluxes. Mar. Ecol. Prog. Ser. **278**: 205–223.
786 Ory, P., H. J. Hartmann, F. Jude, C. Dupuy, Y. Del Amo, P. Catala, F. Mornet, V. Huet, B.
787 Juan, D. Vincent, B. Sautour, and H. Montanié. 2010. Pelagic food web patterns: do
788 they modulate virus and nanoflagellate effects on picoplankton during the
789 phytoplankton spring bloom? Environ. Microbiol., **12 :** 2755-2772
790 Ory, P., Palesse, S., Delmas ,D. and Montanié H., 2011 In situ structuring of virioplancton
791 through bacterial exoenzymatic activity ; interaction with phytoplnkton. Aquatic
792 microbial ecology, **64:** 233-252.
793 Paterson, D.M., R. M. Crawford, and C. Little. 1990. Subaerial exposure and changes in the
794 stability of intertidal estuarine sediments. Est. Coast. Shelf. Sci. **30**:541–556.
795 Paterson, D. M., R. Aspden, and K. S. Black. 2009. Intertidal flats: Ecosystem functioning of
796 soft sediments systems. In: Perillo GME, Wolanski E, Cahoon DR, Brinson MM [ed.],
797 Coastal Wetlands: An Integrated Ecosystem Approach. Elsevier.

798 Pelegri, S. P., J. R. Dolan, and F. Rassoulzadegan. 1999. Use of high temperature catalytic
799 oxidation (HTCO) to measure carbon content of microorganisms. Aquat. Microb. Ecol.
800 **16**: 273–280.
801 Pusceddu, A., C. Fiordelmondo, and R. Danovaro. 2005. Effects on the Benthic Microbial
802 Loop in Experimental Microcosms. Microb. Ecol. **50**: 602–613.
803 Ricard, M., 1987. Atlas du phytoplancton marin, vol. 2. (CNRS, Eds.). Paris.
804 Schmidt, J. L., J. W. Deming, P. A. Jumars, and R. G. Keil. 1998. Constancy of bacterial
805 abundance in surficial marine sediments. Limnol. Oceanogr. **43**: 976–982.
806 Seymour, J. R., L. Seuront, and J. G. Mitchell. 2007. Microscale gradients of planktonic
807 microbial communities above the sediment surface in a mangrove estuary. Est. Coast.
808 Shelf. Sci. **73**: 651–666
809 Sherr, E., B. F. Sherr, and G. A. Paffenhofer. 1986. Phagotrophic protozoa as food for
810 metazoans: a "missing" trophic link in marine pelagic food webs? Mar. Microb. Food
811 Webs **1**:61–80.
812 Sherr, E. B., D. A. Caron, and B. F. Sherr. 1994. Staining of heterotrophic protists for
813 visualisation via epifluorescence microscopy. In: Kemp, PF, Sherr, BF, Sherr, EB, Cole,
814 JJ [ed.], 213–227.Handbook of Methods in Aquatic Microbial Ecology. Lewis
815 Publishers, Boca Raton, FL.
816 Shimeta, J., and J. Sisson. 1999. Taxon-specific tidal resuspension of protists into the subtidal
817 benthic boundary layer of a coastal embayment. Mar. Ecol. Prog. Ser. **177:** 51–62.
818 Shimeta, J, C. L. Amos, S. E. Beaulieu, and O. M. Ashiru. 2002. Sequential resuspension of
819 protists by accelerating tidal flow: Implications for community structure in the benthic
820 boundary layer. Limnol. Oceanogr. **47**: 1152–1164.

Shimeta, J., C. L. Amos, S. E. Beaulieu, and S. L. Katz. 2003. Resuspension of benthic protists at subtidal coastal sites with differing sediment composition. Mar. Ecol. Prog. Ser. **259**: 103–115.

Sournia, A., 1986. Atlas du phytoplancton marin, vol. 1. (CNRS, Eds.). Paris.

Struski, C., and C. Bacher. 2006. Preliminary estimate of primary production by phytoplankton in Marennes-Oleron Bay, France. Est. Coast. Shelf. Sci. **66**: 323–334.

Syngouna, V.I. and Chrysikopoulos, C.V. 2010. Interaction between viruses and clays in static and dynamic bacth system. Environ Sci Technol 44: 4539-4544

Van Duyl, F.C., and A. J. Kop. 1994. Bacterial production in North Sea sediments: clues to seasonal and spatial variations. Mar. Biol. **235**: 323–327.

Widdows, J., M. D. Brinsley, and M. Elliott. 1998. Use of in situ flume to quantify particle flux. 139:85–97, In: Black K.S., Paterson D.M., Cramp A. [ed.], Sedimentary processes in the Intertidal Zone. Geol. Soc. London, Special publication.

Wu, Q. L., Y. Chen, K. Xu, Z. Liu, and M. W. Hahn. 2007. Intra-habitat heterogeneity of microbial food web structure under the regime of eutrophication and sediment resuspension in the large subtropical shallow Lake Taihu, China. Hydrobiologia **581**: 241–254.

Figure 1: Map of the Marennes-Oléron Bay in Europe. The grey area indicates land and the contour labeled 0 delimites the largest extent of the intertidal area (lowest sea level during the highest tidal coefficient). Open circles indicate the successive locations of the Lagrangian survey stations, the open square indicates the Eulerian survey location and the filled triangle indicates the ADV location. Trajectories simulated with the Telemac model are displayed: thin lines figure trajectories reaching the Eulerian survey location at 17:20 h (solid) and 18:40 h (dashed) and the thick line figures trajectory leaving the Eulerian survey location at 16:00 h.

Figure 2: Expected temporal changes in concentrations during a Lagrangian survey (black line) and during a Eulerian survey (gray line) of the water column.

Figure 3: (a) Wind speed at La Rochelle Aérodrome and significant wave height (H_S) on the intertidal flat during high tide (light gray) on 24 July, 2008. (b) Measured bed friction velocities associated with the tidal current (open triangles) and computed bed friction velocities associated with waves in a constant 40 cm water depth during the Lagrangian survey (filled circles for the maximum, open circles for the average) and for water depth increasing from 1.1 to 3.1 m during the Eulerian survey (filled squares for the maximum, open squares for the average).

Figure 4: Temporal changes in concentration of particulate inorganic matter (PIM) in the middle of the water column during the Lagrangian survey (white bar) and during the Eulerian survey (square) at the surface (gray) and at the bottom (white) of the water column. The black vertical bar represents the average concentration in the middle of the water column in the lower part of the mudflat when surveys started with its 80% confidence interval. Lines display the 80% confidence interval of concentrations calculated assuming only mixing with

incoming offshore waters when tide rose during the Eulerian survey (see formula in the Methods section).

Figure 5: Temporal changes in the abundances of autotrophic organisms: benthic diatoms (a), pelagic diatoms (b), autotrophic nanoflagellates (ANF, c), Picophytoeukaryots (d) and *Synechococcus* (e) in the middle of the water column during the Lagrangian survey (white bar) and during the Eulerian survey (square) at the surface (gray) and at the bottom (white) of the water column. The black vertical bar represents the average concentration in the middle of the water column in the lower part of the mudflat when surveys started with its 80% confidence interval. Lines display the 80% confidence interval of concentrations calculated assuming only mixing with incoming offshore waters when tide rose during the Eulerian survey (see formula in the Methods section).

Figure 6: Temporal changes in the abundances of heterotrophic organisms: free viruses (a), free bacteria (b), attached bacteria (c), heterotrophic nanoflagellates (HNF, d) and ciliates (e) in the middle of the water column during the Lagrangian survey (white bar) and during the Eulerian survey (square) at the surface (gray) and at the bottom (white) of the water column. The black vertical bar represents the average concentration in the middle of the water column in the lower part of the mudflat when surveys started with its 80% confidence interval. Lines display the 80% confidence interval of concentrations calculated assuming only mixing with incoming offshore waters when tide rose during the Eulerian survey (see formula in the Methods section).

Figure 7: Temporal trends in the autotrophs (a) and heterotrophs (b) biomass in the middle of the water column during the Lagrangian survey (white bar) and during the Eulerian survey (square) at the surface (gray) and at the bottom (white) of the water column. The black

vertical bar represents the average concentration in the middle of the water column in the lower part of the mudflat when surveys started with its 80% confidence interval.

Table 1: Concentrations of parameters at the north station on July 12 and 29, 2008, used as offshore value C_{ext} in equation (1).

	July 12 / July 29
PIM	18.2 / 6.67 mg L^{-1}
Pelagic diatoms	112.7 / 52.8 cell mL^{-1}
Benthic diatoms	17.3 / 4.2 cell mL^{-1}
ANF	1.8 / 1.0 10^3 cell mL^{-1}
Picoeukaryots	5.5 / 2.88 10^3 cell mL^{-1}
Synechococcus sp.	1.44 / 2.25 10^4 cell mL^{-1}
Free virus	3.8 / 2.34 10^6 cell mL^{-1}
Free bacteria	2.65 / 2.48 10^6 cell mL^{-1}
Attached bacteria	5.3 / 7.5 10^3 cell mL^{-1}
HNF	1.5 / 0.6 10^3 cell mL^{-1}
Ciliates	3.66 / 4.58 cell mL^{-1}

Table 2: Conversion factors and their corresponding literature reference used to convert abundance to biomass of carbon for each type of plankton organism.

Cells or organism	**Conversion factor (pg C/cell)**	**Reference**
Bacteria	0.016	Labry et al. (2002)
Synechococcus	0.104	Blanchot and Rodier (1996)
Picoeukaryotes	0.104	Blanchot and Rodier (1996)
Nanoflagellates	3.14	Pelegri et al. (1999)
Ciliates	3.14	Pelegri et al. (1999)
Diatoms	225	Fournier et al. (2012)

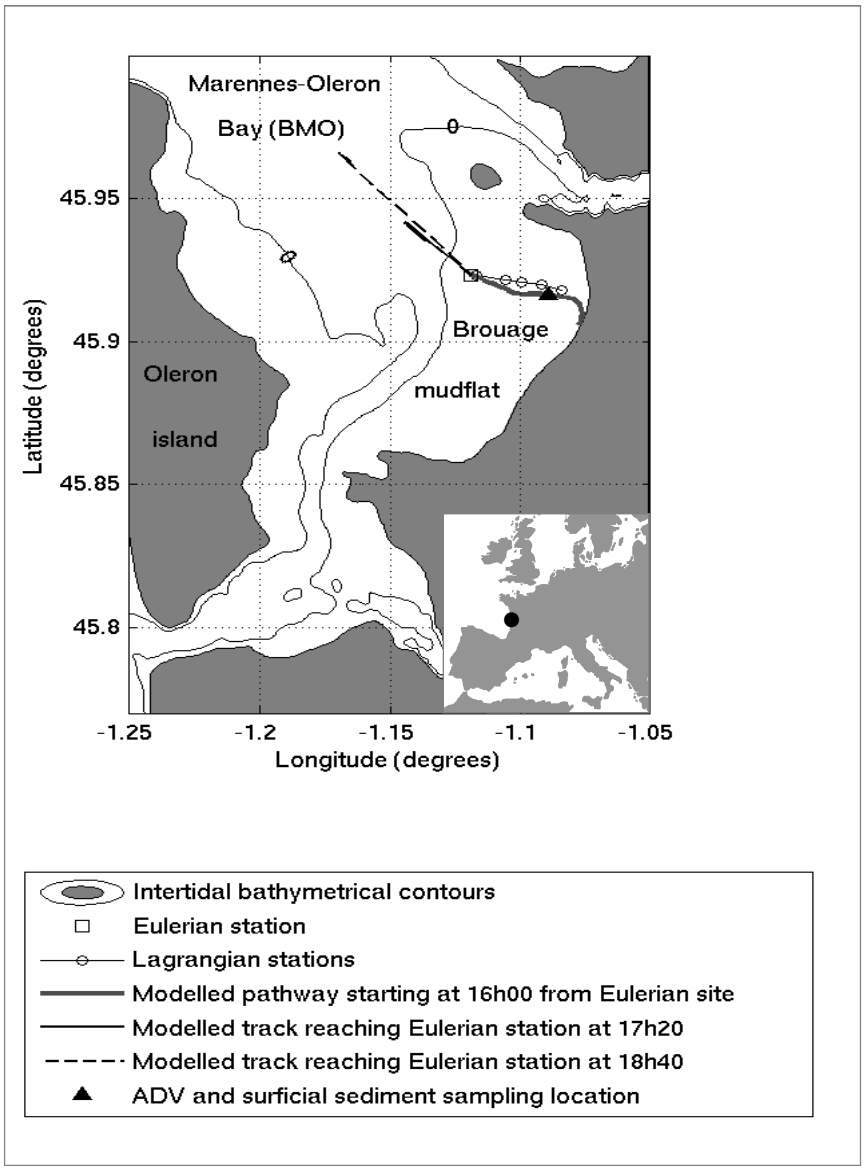
Marennes-Oleron
Bay (BMO)
Brouage
mudflat
Oleron
island
45.95
45.9
45.85
45.8
-1.25
-1.2
-1.15
-1.1
-1.05
Latitude (degrees)
Longitude (degrees)
Intertidal bathymetrical contours
Eulerian station
Lagrangian stations
Modelled pathway starting at 16h00 from Eulerian site
Modelled track reaching Eulerian station at 17h20
Modelled track reaching Eulerian station at 18h40
ADV and surficial sediment sampling location

Figure 1

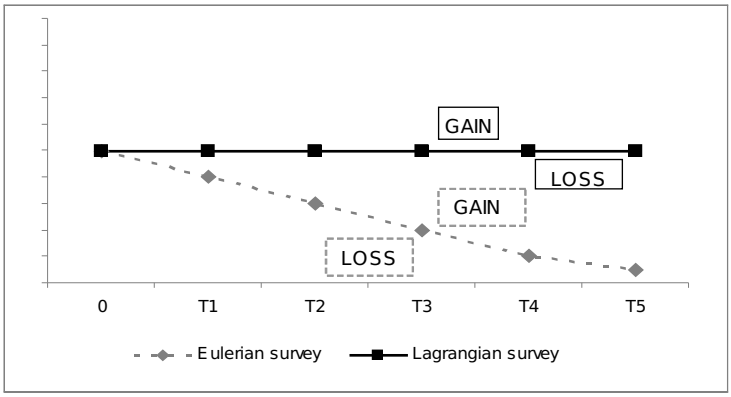
GAIN
LOSS
GAIN
LOSS
0
T1
T2
T3
T4
T5
Eulerian survey
Lagrangian survey

Figure 2

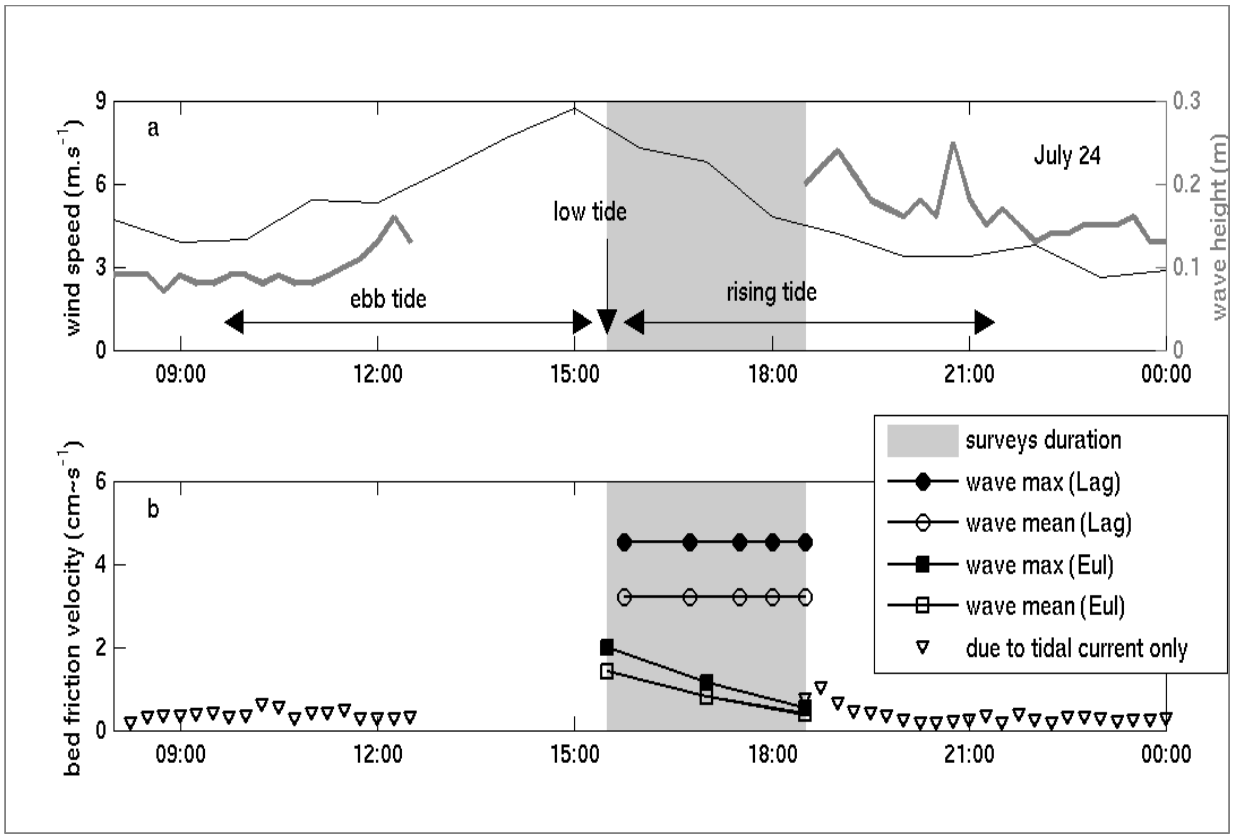
a
wind speed (m.s-1)
wave height (m)
July 24
low tide
ebb tide
rising tide
09:00
12:00
15:00
18:00
21:00
00:00
b
bed friction velocity (cm~s-1)
surveys duration
wave max (Lag)
wave mean (Lag)
wave max (Eul)
wave mean (Eul)
due to tidal current only

Figure 3

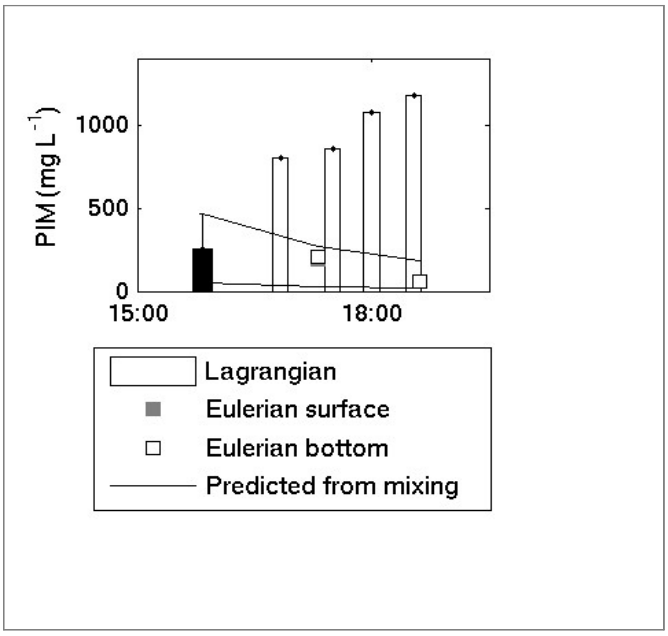
PIM (mg L^{-1})
1000
500
0
15:00
18:00
Lagrangian
Eulerian surface
Eulerian bottom
Predicted from mixing

Figure 4

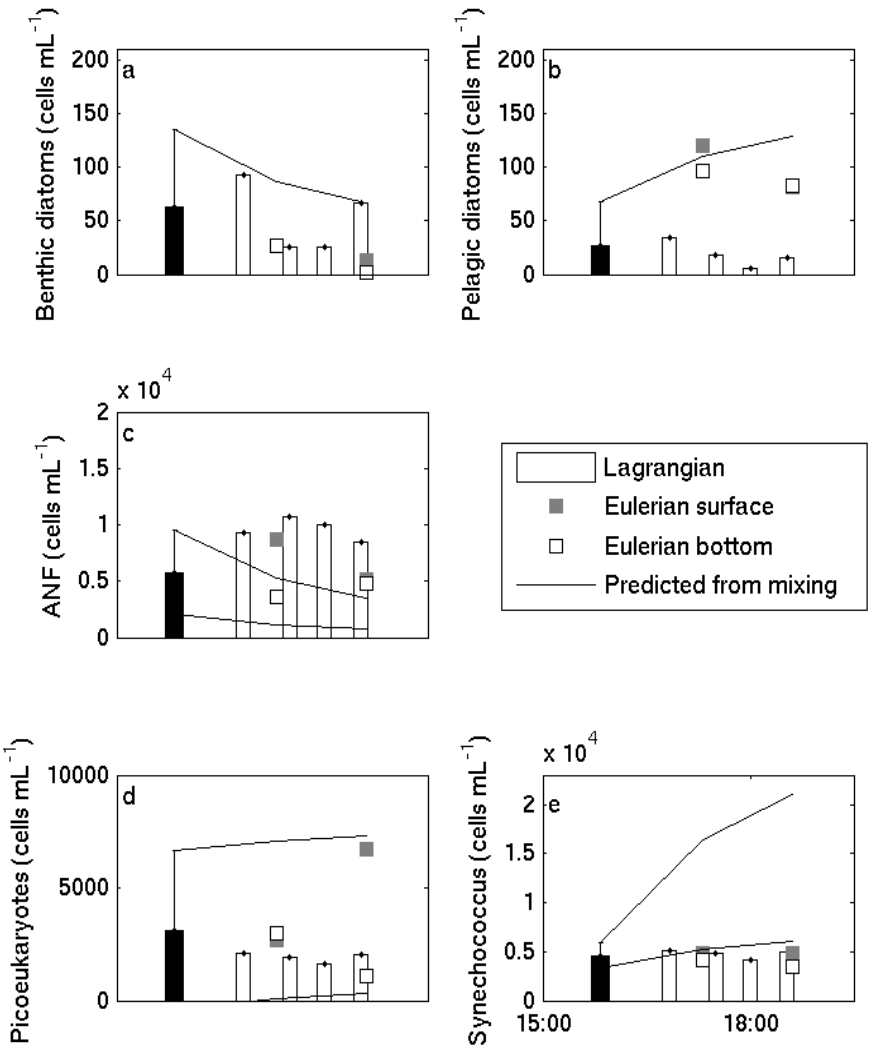
Benthic diatoms (cells mL-1)
a
Pelagic diatoms (cells mL-1)
b
x 10^4
ANF (cells mL-1)
c
Lagrangian
Eulerian surface
Eulerian bottom
Predicted from mixing
Picoeukaryotes (cells mL-1)
d
x 10^4
Synechococcus (cells mL-1)
e
15:00
18:00

Figure 5

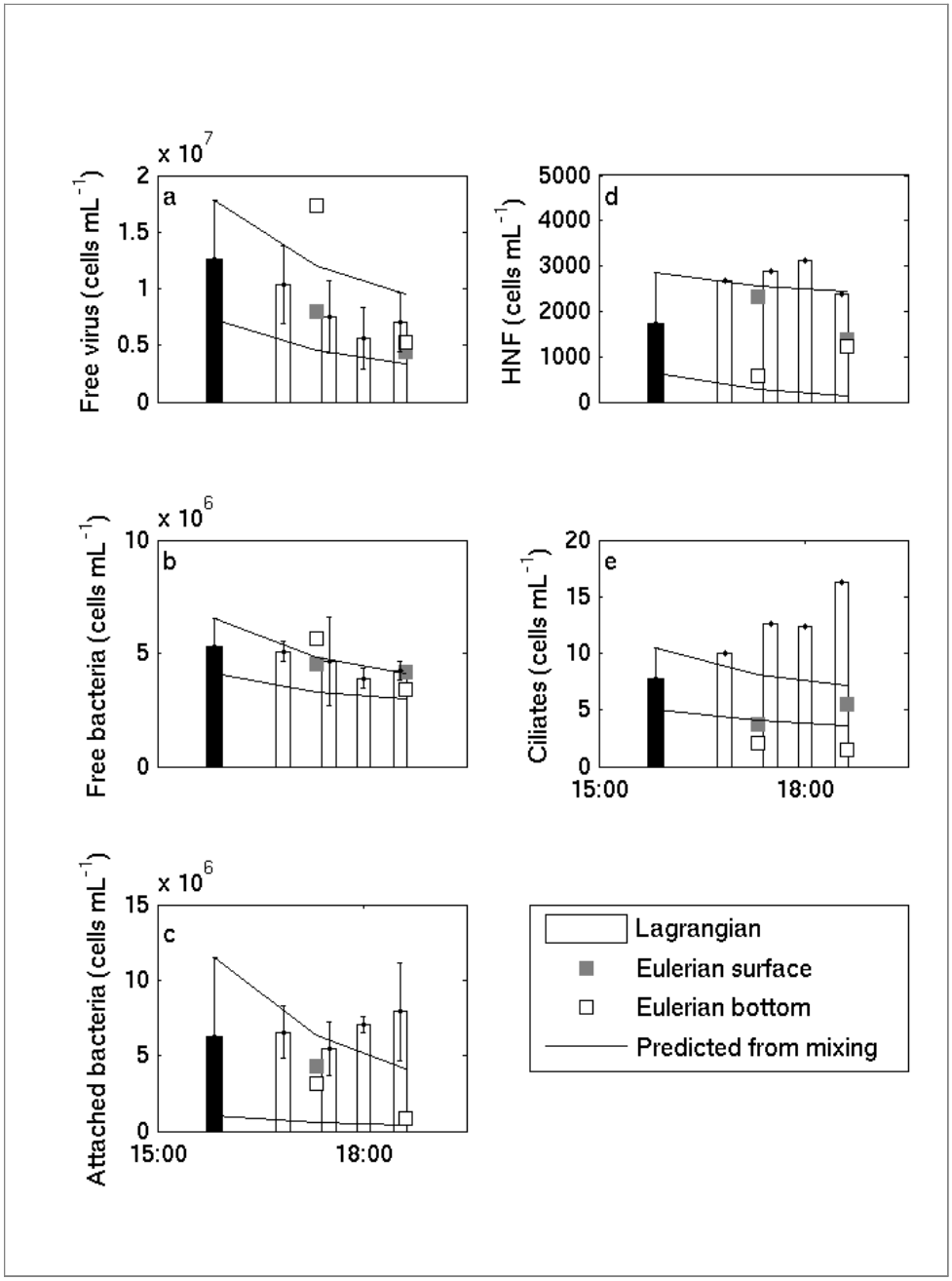
x 10^7
a
Free virus (cells mL^-1)
2
1.5
1
0.5
0
d
HNF (cells mL^-1)
5000
4000
3000
2000
1000
0
x 10^6
b
Free bacteria (cells mL^-1)
10
5
0
e
Ciliates (cells mL^-1)
20
15
10
5
0
15:00
18:00
x 10^6
c
Attached bacteria (cells mL^-1)
15
10
5
0
15:00
18:00
Lagrangian
Eulerian surface
Eulerian bottom
Predicted from mixing

Figure 6

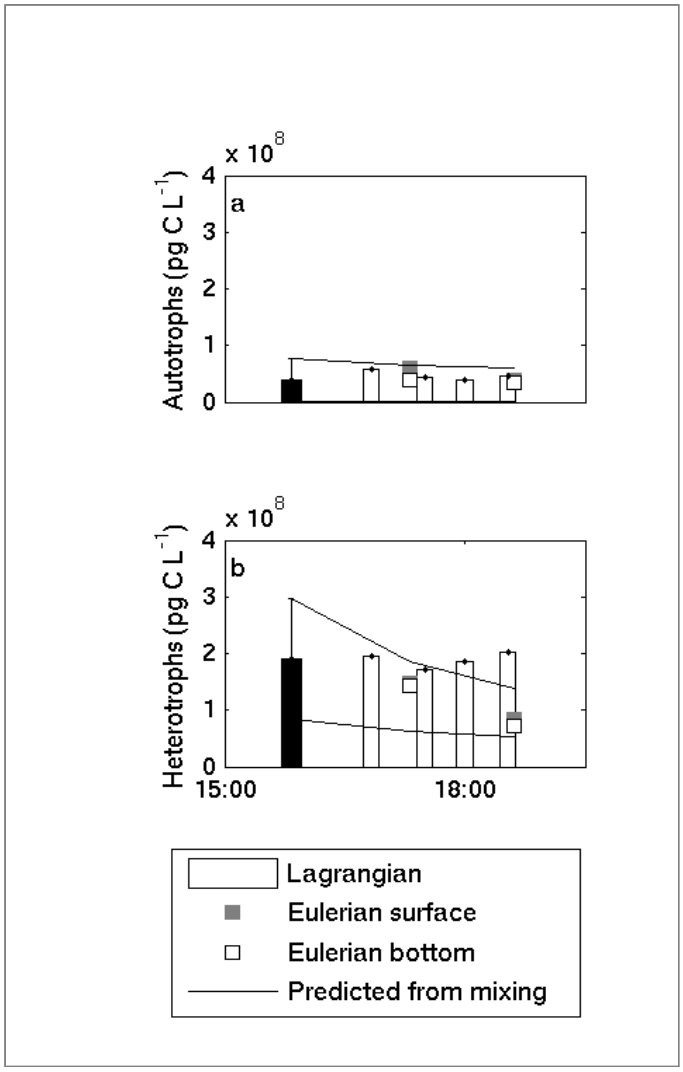
x 10^8
a
Autotrophs (pg C L^-1)
4
3
2
1
0
x 10^8
b
Heterotrophs (pg C L^-1)
4
3
2
1
0
15:00
18:00
Lagrangian
Eulerian surface
Eulerian bottom
Predicted from mixing

Figure 7